

Spatiotemporal dynamics of bacterial populations in the anoxic Cariaco Basin

Xueju Lin¹ and Mary I. Scranton

Marine Sciences Research Center, Stony Brook University, Stony Brook, New York 11794

Andrei Y. Chistoserdov

Department of Biology, University of Louisiana at Lafayette, Lafayette, Louisiana 70504

Ramon Varela

Estacion de Investigaciones Marinas de Margarita, Fundacion La Salle de Ciencias Naturales, Apartado 144, Punta de Piedras, Edo. Nueva Esparta, Venezuela

Gordon T. Taylor

Marine Sciences Research Center, Stony Brook University, Stony Brook, New York 11794

Abstract

Distributions of bacterial populations in the anoxic Cariaco Basin were studied over 2 yr (five cruises) at three stations using fluorescence in situ hybridization (FISH) and terminal restriction fragment length polymorphism (T-RFLP) of 16S ribosomal ribonucleic acid (rRNA) genes. FISH results demonstrate that the contribution of ϵ -proteobacterial abundances to total prokaryotic inventories was relatively constant among cruises, and this group was dominant in the redoxcline, accounting for 18% of DAPI (4',6-diamidino-2-phenylindole)-stained counts on average. In contrast, β -proteobacteria were more variable. Sulfate reducers, α -, and γ -proteobacteria accounted for minor components of the anaerobic microbial communities. T-RFLP fingerprinting also showed significant temporal shifts in bacterial community composition. The greatest variations in bacterial community structure were evident among oxic, transitional, and anoxic zones, but significant horizontal variations were also evident within redoxclines of three different stations. A statistical analysis of T-RFLP patterns revealed clear spatiotemporal patterns in bacterial community structure along the redox gradient among sites and over time. Total prokaryotic abundances corresponded well with seasonal variations in organic carbon fluxes above the redoxcline. However, no single measured environmental variable (O_2 , H_2S , $S_2O_3^{2-}$, H_4SiO_4 , NO_3^- , PO_4^{3-} , microbial biomass, chemoautotrophic production) explained the temporal oscillations of the dominant bacterial groups. Analyses suggest that redox gradients, terrestrial inputs, and disturbance due to lateral intrusions of adjacent waters could significantly affect bacterial community composition in the Cariaco Basin.

¹ Corresponding author. Present address: Stroud Water Research Center, 970 Spencer Road, Avondale, Pennsylvania 19311, (xlin@stroudcenter.org).

Acknowledgments

We thank the captain and crew of the B/O *Hermano Gines* and the staff of the Fundacion La Salle de Ciencias Naturales for their assistance during our fieldwork in Venezuela. We are grateful to D. Percy for providing the sulfur data, and M. J. Rodriguez for assistance in DNA collection. Nutrient samples were analyzed in the laboratory of Kent Fanning (University of South Florida). Our deepest appreciation also goes to the following colleagues for their collaboration and data: Frank Muller-Karger and Laura Lorenzoni (University of South Florida), Robert Thunell and Claudia Benitez-Nelson (University of South Carolina). We are also indebted to J. Collier and M. Doall for assistance with T-RFLP analyses, which were performed in the National Science Foundation-funded MEAD Laboratory in the Department of Ecology and Evolution at Stony Brook University. We would like to thank two anonymous reviewers for their helpful comments on the manuscript.

This research was supported by grants from the National Science Foundation (OCE-03-26175 and MCB03-47811 to G.T.T., M.I.S., and A.Y.C.) and from Venezuela FONACIT (Fondo Nacional de Ciencia, Tecnología e Investigación) (2000001702). This is Marine Sciences Research Center contribution 1342.

To date, temporal changes in the biogeochemistry of the Cariaco Basin have been fairly well studied (Muller-Karger et al. 2001; Scranton et al. 2001; Astor et al. 2003). Biological variables, such as primary production, microbial biomass, and midwater dark CO_2 fixation, vary with seasonal shifts of local upwelling intensity, regional fluvial discharge, trade-wind intensity, and lateral intrusions of oxic waters, among other factors (Muller-Karger et al. 2001; Taylor et al. 2001; Astor et al. 2003). Molecular genetic characterizations of the microbial communities of several anoxic systems have revealed active and diverse microbial communities varying along strong vertical gradients of redox-sensitive elements in the water column (Vetriani et al. 2003; Labrenz et al. 2005; Lin et al. 2006). However, temporal dynamics of phylogenetic and functional bacterial assemblages across oxic–anoxic transitions have not been reported and related to environmental conditions. In fact, no convincing evidence from empirical studies so far has been able to consistently connect diversity with functional processes (Madsen 2005; Konopka 2006), although a recent time-series study by Fuhrman et al. (2006) showed that annually recurring bacterial communities are predictable from ocean conditions. One outstanding question about marine microbial distributions is

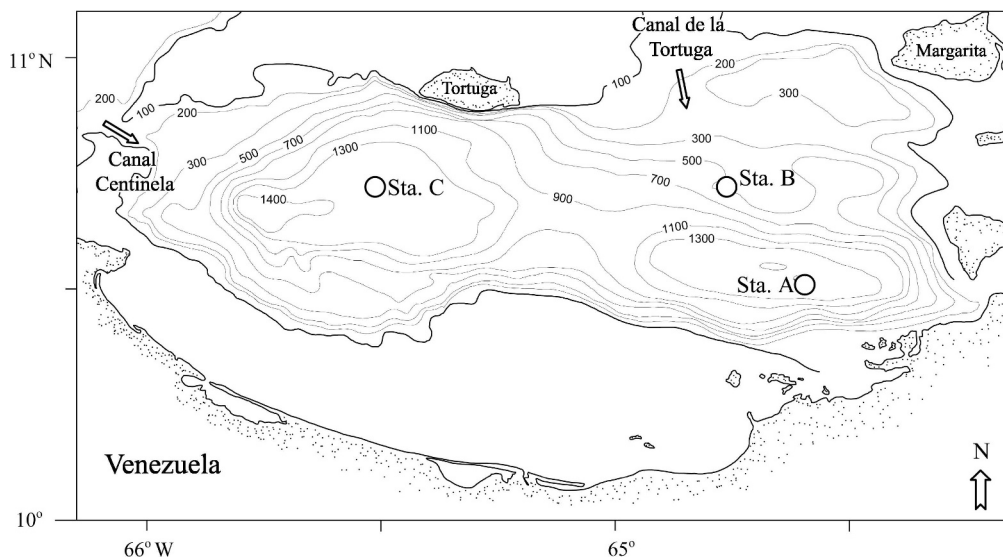


Fig. 1. Map of the Cariaco Basin with stations indicated by circles. Isobaths are in meters. Arrows indicate pathways for water intrusion from the Caribbean Sea.

whether long-term variability of marine microbial communities can be understood by intermittent sampling and community snapshots (Hunter-Cevera et al. 2005). Here, we took advantage of the CARIACO (CARbon Retention In A COlored Ocean) time-series program and used bacterial assemblages along redox gradients as our model community to map bacterial populations onto the geochemical “landscape.” We believe that understanding the primary drivers of bacterial diversity and the temporal and vertical changes to community composition along redox gradients can lend insight into functional roles of bacterial populations that are difficult to study *in situ*.

To pursue our goal, we employed fluorescence *in situ* hybridization (FISH) and terminal restriction fragment length polymorphism (T-RFLP) of bacterial 16S ribosomal ribonucleic acid (rRNA) genes to characterize bacterial community composition over 2 yr along redox gradients in the Cariaco system. Generally, “aquatic microbial communities” are considered to be theoretical constructs rather than real ecological entities with well-constrained structure, common genome, or evolutionary history (Perntaler and Amann 2005). For practical purposes, a bacterial population in this paper is defined as an assemblage of individuals sharing a high degree of genotypic similarity and being reliably identified and quantified by FISH or T-RFLP techniques. The limited array of molecular FISH probes obviously does not permit determination of highly resolved community structure. However, sequencing and probing 16S ribosomal RNA genes have revealed that Cariaco microbial communities are dominated by Bacteria, especially proteobacteria, although Archaea can be common within the Cariaco’s redoxcline (Madrid et al. 2001; Lin et al. 2006). These previous and other results suggest that selected probes specific for five subdivisions of proteobacteria are sufficient for monitoring major population dynamics within the bacterioplankton (Giovannoni et al. 1996).

Top-down controls on bacterial community composition in the Cariaco redoxcline have been explored recently (Lin et al. 2007). In this paper, we focus on bottom-up drivers of spatiotemporal dynamics within bacterial communities in the Cariaco redoxcline. Geochemical data, including environmental variables (concentrations of O_2 , H_2S , $S_2O_3^{2-}$, H_4SiO_4 , NO_3^- , PO_4^{3-} , SO_4^{2-} , NH_4^+ , NO_2^- , and rates of chemoautotrophic, and heterotrophic production) and organic carbon and terrigenous material flux into sediment traps, were obtained from collaborating laboratories. Multivariate statistical analyses were used to explore potential connections between bacterial community composition and environmental variables.

Methods

Field site, sampling, and biogeochemical measurements—The Cariaco system is located on the northern continental shelf of Venezuela in the Caribbean Sea (Fig. 1) and is the second largest permanently anoxic marine water body in the world (Richards 1975; Muller-Karger et al. 2001). The system consists of western and eastern basins, connected by a saddle rising to a depth of 900 m. Circulation in the deeper basin is restricted by sills at about 90–120-m depth along the system’s northern and western boundary. Surface waters between the Cariaco system and the Caribbean Sea exchange through Canal Centinela and Canal de la Tortuga (Fig. 1). The time-series stations, Sta. A (1,400 m, 10.30°N, 64.40°W) and Sta. C (1,400 m, 10.40°N, 65.35°W), are situated in the eastern and western sub-basin of the Cariaco system, respectively. To explore possible effects of oxic water intrusion on biogeochemical processes, we also sampled Sta. B (400 m, 10.40°N, 64.46°W), which is located between Sta. A and the Canal de la Tortuga.

Collection depths were selected to consistently capture the same features of the redoxcline (250–400 m) during each cruise. Bacterioplankton samples were collected at 18

depths during early (Jan) and late (May) upwelling seasons, including 08 May 2003 (CAR-89), 21 Jan 2004 (CAR-96), 18 May 2004 (CAR-100), 17–18 Jan 2005 (CAR-108), and 23–24 May 2005 (CAR-112) at the time-series stations. During the CAR-112 cruise, all three stations were sampled to examine spatial variations of bacterial community composition. Samples for FISH were withdrawn from 8-liter Teflon-coated Niskin bottles under N₂ atmosphere and fixed overnight with borate-buffered and filtered (0.22 μm) formaldehyde solution (final concentration 2% [v/v]). Cells from duplicate 20–60-mL samples were collected on white polycarbonate membranes (Millipore, type GTTP, 0.2-μm pore size, 47-mm diameter), washed with 20 mL of sterile distilled water, and stored at –20°C.

For genomic deoxyribonucleic acid (DNA) samples, 2–4 liters of water, were collected during cruises CAR-96 (270, 280, 320 m) and CAR-100 (265, 290, 312 m) by filtration onto 0.22-μm Durapore filters (Millipore) that were immersed in lysis buffer (400 mmol L⁻¹ NaCl, 750 mmol L⁻¹ sucrose, 20 mmol L⁻¹ EDTA (ethylenediaminetetraacetic acid) [pH 7.4], 50 mmol L⁻¹ Tris-HCl [pH 9.0]), stored at –20°C in the field, and transferred to –80°C freezer for long-term storage. For CAR-108 and 112 cruises, triplicate 60-mL water samples were filtered through 0.2-μm pore-size, 13-mm Millipore Express[®] membranes (type GPWP) in Swinnex 13[®] filter holders (Millipore) using a polypropylene syringe. Filters were placed in 0.6-mL sterile microcentrifuge tubes, immersed in 180 μL of DNA lysis buffer (20 mmol L⁻¹ Tris-HCl [pH 8.0], 2 mmol L⁻¹ EDTA [pH 8.0], 1.2% Triton X-100) and stored at –20°C before DNA extraction. To evaluate potential biases in community composition estimated from 60-mL samples, bacterioplankton from larger water samples (1–4 liters) were collected in parallel during the CAR-108 cruise.

Discrete samples for O₂, H₂S, nutrients, thiosulfate, heterotrophic, and chemoautotrophic production were taken from the same Niskin bottles. Details of these methods have been described previously (Taylor et al. 2001; Scranton et al. 2006; Percy et al. in press). Organic carbon and terrigenous material fluxes were determined from sediment traps deployed at 225, 405, 840, and 1,200 m by R. Thunell group (unpubl. data). Standard DAPI (4′-diamidino-2-phenylindole)-stained slides were prepared with 5–20 mL of seawater on dark 0.2-μm pore-size Poretics polycarbonate membrane for enumeration of total prokaryotes (Porter and Feig 1980).

Fluorescence in situ hybridization with oligonucleotide probes—The following oligonucleotide probes were employed in our samples: EUB338 (5′-GCT GCC TCC CGT AGG AGT-3′, specific for domain Bacteria; Amann et al. 1990); ALF968 (5′-GGT AAG GTT CTG CGC GTT-3′, specific for the α-proteobacteria; Neef 1997); BET42a (5′-GCC TTC CCA CTT CGT TT-3′, specific for the β-proteobacteria; Manz et al. 1992); GAM42a (5′-GCC TTC CCA CAT CGT TT-3′, specific for the γ-proteobacteria; Manz et al. 1992); SRB385 (5′-CGG CGT CGC GTC AGG-3′, most sulfate reducers of δ-proteobacterial affiliation; Amann et al. 1990); EPS549 (5′-CAG TGA TTC CGA GTA ACG -3′, specific for the ε-proteobacteria; Lin

et al. 2006); EPS682 (5′-CGG ATT TTA CCC CTA CAC-3′, improved probe for the ε-proteobacteria; Lin et al. 2007); and NONEUB (5′-ACT CCT ACG GGA GGC AGC-3′, nonsense sequence used as a negative control; Wallner et al. 1993). The probe BETA2-870 (5′-CCC AGG CGG CTG ACT TCA-3′, specific for some of β-proteobacteria; Burkert et al. 2003) was used to target a cosmopolitan freshwater lineage of β-proteobacteria from Sta. A samples from the cruise CAR112 and to determine if β-proteobacteria in the Cariaco Basin were from freshwater systems. For samples analyzed after the CAR-108 cruise, we replaced EPS549 with EPS682 due to higher hybridization efficiency of EPS682 (Gibbs free energy change = –12.5 kcal mol⁻¹) compared with EPS549 (Gibbs free energy change = –9.0 kcal mol⁻¹). Gibbs free energy change is a proxy for probe hybridization efficiency and was calculated according to Yilmaz and Noguera (2004). Usually, a threshold value of –13.0 kcal mol⁻¹ Gibbs free energy change is recommended for effective probe hybridization. All probes were commercially synthesized and labeled with the indocarbocyanine dye CY3 by Thermo-Hybrid (Interactiva Division, Ulm, Germany) or Integrated DNA Technologies Inc. Specificity and hybridization conditions are summarized elsewhere (Lin et al. 2006).

The subdomain level probes selected in this study covered 73–113% (mean = 96%) of EUB338-positive cells, which accounted for an average 74% of total prokaryotes (DAPI-positive) in the Cariaco Basin (Lin et al. 2006). Due to the labor-intensive nature of the FISH technique, we only applied NONEUB, EUB338, BET42a, and EPS495/682 probes to samples from all five cruises. The ALF968, GAM42a, and SRB385 probes were selectively applied to samples from CAR-96, CAR-108, and CAR-112 cruises that captured time periods when β-proteobacteria were prevalent (CAR-89, 96, and 112) or rare (CAR-100 and 108). Bacteria targeted by these three probes were only minor contributors to total prokaryotic inventories in Cariaco samples. In addition, the CF319 probe (Manz et al. 1996) was employed only for the CAR-96 samples, because this bacterial group was a minor contributor in our previous Cariaco study (Lin et al. 2006).

Procedures for FISH experiments have been described in detail previously (Lin et al. 2006). FISH with catalyzed reporter deposition (CARD-FISH) was used with the EPS549 probe for CAR-89, 96, 100, and 108 samples. All other measurements were performed according to oligo-FISH protocol. Details of our specific procedures for oligo-FISH and CARD-FISH and their optimization have been described elsewhere (Lin et al. 2006). Potential method disparities for ε-proteobacterial detection were evaluated with samples from Sta. A during the CAR-108 cruise. Abundances of ε-proteobacteria detected by CARD-FISH with the EPS549 probe were not significantly different from those detected by oligo-FISH with the EPS682 probe (*t*-test, *n* = 14, *p* = 0.49). Therefore, results for ε-proteobacteria obtained by either method appear to be comparable, and the method used does not appear to influence our cruise-to-cruise comparisons.

Briefly, for FISH analysis, each 47-mm membrane filter was cut into 16 wedges. Individual wedges were covered

with 50 μL of hybridization solution containing 0.9 mol L^{-1} NaCl, 20 mmol L^{-1} Tris-HCl (pH 7.5), 0.01% sodium dodecylsulfate (SDS), 35% formamide, and 2.5 ng μL^{-1} of CY3-labeled oligonucleotide, and then samples were incubated at 46°C for 2 h in the humidity-equilibrated chamber of an InSlide-Out® hybridization oven (Boeckel Scientific). After hybridization, filter wedges were quickly transferred to a prewarmed (48°C) vial containing 50 mL of washing solution (80 mmol L^{-1} NaCl, 20 mmol L^{-1} Tris-HCl (pH 7.4), 5 mmol L^{-1} EDTA, and 0.01% SDS) and incubated without agitating at 48°C for 30 min. Filter wedges were dried on Whatman 3M blotting paper and mounted on slides with Citifluor AF1 containing 1.0 $\mu\text{g mL}^{-1}$ DAPI. Slides were stored in the dark at -20°C and examined using a Zeiss Axioskop epifluorescence microscope equipped with an HBO 50 W Hg vapor lamp, appropriate filter sets for CY3 and DAPI dyes, a 100 \times objective, an Optronics MagnaFire CCD camera, and ImagePro 4.5 image-analysis system. More than 20 fields or 500 DAPI-stained cells were counted per filter section.

DNA extraction—Two protocols were employed for DNA extraction and purification. For large-volume filtrations, DNA was extracted according to Moeseneder et al. (1999). Briefly, Durapore membranes (47 mm) containing bacterial communities stored frozen in 2 mL of lysis buffer were incubated with lysozyme (final 1 mg mL^{-1} ; Roche Molecular Systems) at 37°C for 30 min. Twenty microliters of DNase-free RNase I (500 $\mu\text{g mL}^{-1}$; Roche Molecular Systems) was then added, and the sample was incubated at 37°C for 30 min. Sodium dodecyl sulfate (SDS) (final concentration 1% [wt/vol]) and proteinase K (final concentration 100 $\mu\text{g mL}^{-1}$) were then added, and the sample was incubated at 55°C for 2 h. The lysate was checked under a microscope for complete lysis of the bacterial cells. At this point, membranes were removed from tubes and washed with 600 μL TE (10 mmol L^{-1} Tris-HCl [pH 8.0], 1 mmol L^{-1} EDTA). Lysate was extracted with an equal volume of phenol-chloroform-isoamyl alcohol (25:24:1), shaken and vortexed gently. Tubes were centrifuged (4,500 $\times g$) for 5 min at room temperature. The aqueous layer (DNA-bearing) was carefully transferred to a new sterile tube and extracted once with an equal volume of chloroform-isoamyl alcohol (24:1). After mixing and spinning, the aqueous layer was transferred to a new tube, and nucleic acids were precipitated by the addition of 1/10 volume 3 mol L^{-1} sodium acetate (pH 5.2) and 2.5 volumes of 99.6% ethanol. The mixture was stored overnight at -20°C, and then centrifuged (12,000 $\times g$) for 15 min at 4°C. Pellets were dissolved in 1 mmol L^{-1} TE and incubated at room temperature for 10 min. DNA was further purified using the Qiaex II extraction kit according to the manufacturer's manual (Qiagen).

For small-volume water samples, filters in microcentrifuge tubes were thawed and incubated with 20 mg mL^{-1} lysozyme for 1 h at 37°C (Suzuki et al. 2001). Subsequently 1 μL of 500 $\mu\text{g mL}^{-1}$ DNase-free RNase I (Roche Molecular Systems) was added and samples were incubated for 5 min at room temperature. Twenty-five microliters of

Proteinase K (25 mg mL^{-1}) were then added, and samples were subsequently treated according to the DNeasy® tissue kit protocol for gram-positive bacteria (Qiagen) to guarantee complete lysis of both gram-negative and gram-positive bacteria. Extracts from triplicate samples were pooled to limit effects of random filtration and extraction bias. We recognize that 2–4-liter samples may represent total community diversity more accurately than 60-mL samples; however, for ecological studies, there are trade-offs between sample size and number of samples processed (McCune and Grace 2002). Generally, the “many-but-small” strategy will yield relatively accurate abundance estimates for the most common taxa but will yield an incomplete species list (McCune and Grace 2002). The “large-but-few” strategy will yield a relatively complete species list but will tend to overestimate the cover of rarer taxa and yield imprecise estimates of the more common taxa. In fact for samples from three depths (250 m, 270 m, and 310 m) during the CAR-108 cruise, there were no significant differences in either peak numbers or T-RFLP patterns (relative areas of peaks) between large-volume DNA samples and small-volume ones (*t*-test, *n* = 29, *p* = 0.74).

Polymerase chain reaction (PCR) and T-RFLP analysis—The bacteria-specific primers used for PCR amplification of 16S rRNA genes were 63F-FAM (5'-CAG GCC TAA CAC ATG CAA GTC-3') and 778R (5'-AGG GTA TCT AAT CCT GTT TGC-3') (Marchesi et al. 1998). 63F-FAM was 5'-end labeled with phosphoramidite fluorochrome 5-carboxyfluorescein (Integrated DNA Technologies). PCR mixtures (50 μL final volume) contained 1 \times PCR buffer (Stratagene), 250 $\mu\text{mol L}^{-1}$ of each deoxynucleoside triphosphate (Roche Molecular Systems), 200 nmol L^{-1} primers, and 1.25 units of SureStart *Taq* DNA polymerase (Stratagene). An approximate 1 ng quantity of DNA from samples was added to each PCR reaction. PCR was performed in a Stratagene Mx3000p thermal cycler with an initial denaturation step of 95°C for 10 min, followed by 30 cycles of 95°C for 30 s, 55°C for 30 s, and 72°C for 1 min, and a final extension at 72°C for 7 min. Five replicate PCR products per sample were pooled and purified with a QIAquick PCR purification kit (Qiagen) according to the manufacturer's instructions. Amplification products were visualized by electrophoresis through a 1.0% agarose gel in 1 \times TAE (40 mmol L^{-1} Tris-acetate, 1 mmol L^{-1} EDTA) containing ethidium bromide (0.50 mg mL^{-1}). Concentrations of PCR products were measured fluorometrically by PicoGreen staining (Molecular Probes) with a Fluorescence HPLC monitor (RF-551, Shimadzu) according to the manufacturer's specifications.

Restriction digests were standardized and replicated by using 100 ng of purified PCR product for each sample. Digests were performed with the restriction endonuclease *Alu* I (AG/CT) (Promega) and associated buffers under conditions recommended by the manufacturer. Digestions were conducted for 6 h with *Alu* I at 37°C. After ethanol precipitation, the fragment mixtures were dissolved in 10 μL of PCR-grade water (Roche Molecular Systems).

Prior to capillary electrophoresis, subsamples (5 μL) were mixed with Hi-Di formamide (10 μL) and a MapMarker[®] Rox1000 size standard (0.5 μL) (Bioventure). Analysis of 5 μL of this mixture was performed in an ABI 3100 capillary electrophoresis system. In silico enzyme resolution power analysis was performed with the MiCA 3 online tool (<http://mica.ibest.uidaho.edu/enzyme.php>). Compared with several widely used restriction endonucleases, such as *Hha* I, *Msp* I, *Rsa* I, and *Mvn* I, *Alu* I has the most successful hits against bacterial 16S rRNA sequences in RDP II database as assessed by the MiCA 3 online analysis tool. In our *Alu* I digests, no fragments more than 400 base pairs (bp) were observed in T-RFLP profiles in any sample. However, several 700 bp fragments appeared in digests by *Msp* I and *Rsa* I in all our samples, indicating that no restriction sites were targeted by these two enzymes in some Cariaco bacterial 16S rRNA sequences.

Data processing—Based on the zonation of biogeochemical properties (e.g., electron donors and acceptors), we divided the Cariaco water column into three zones: oxic (0–250 m), redoxcline (250–400 m), and anoxic (400–1,300 m). Temporal variations in bacterial populations determined by FISH were assessed based on averaged values of relative abundances of specific bacterial groups within each zone. Disparity in potential density (kg m^{-3} , $\Delta\rho = \rho_x - \rho_{x-1}$, where x is a cruise number) between consecutive cruises at Sta. A was used as an indicator for lateral intrusions of Caribbean midwater mass from outside the Cariaco Basin. Here, we assumed that the Caribbean midwater mass was denser than waters in the Cariaco redoxcline. Therefore, a positive $\Delta\rho_{x-(x-1)}$ value means occurrence of a lateral intrusion event prior to the cruise x . Data for the potential density were obtained from the Cariaco website: <http://www.imars.usf.edu/CAR/index.html>.

Electropherograms were analyzed with GeneMapper v3.7 software (ABI) for fragment lengths of between 30 and 500 bp with a minimum peak height threshold of 50 fluorescence units. Sample profiles with cumulative peak heights less than 10,000 total fluorescence units were discarded, and samples were rerun (Blackwood et al. 2003). Peak patterns from different samples were manually aligned by size sorting and manually grouping peaks within one base of fragment length. Peaks occurring only in one of two replicates at any depth were deleted from the data. These peaks were usually considered as single-stranded pseudofragments and were less than 8% of total identified peaks per sample. Peak areas were normalized based on their proportion to total area of each T-RFLP profile. The term operational taxonomic unit (OTU) is used to represent individual restriction fragments in T-RFLP patterns, and each OTU in this case may be a combination of more than one distinct bacterial ribotype. We recognize that analysis of absence/presence data in ordinations may reduce effects of PCR bias. However, other studies together with our data show that results from proportional peak area data are not significantly different from those based on absence/presence data (Blackwood et al. 2003; Pett-Ridge and Firestone 2005). Compared with absence/presence matrices of OTUs, matrices with normalized peak

data can more approximately reflect diversity (ribotype richness as well as ribotype evenness).

Statistical analyses—T-RFLP patterns from the *Alu* I digest were converted to a matrix using relative percent area and analyzed with PC-ORD v4 (MjM Software Design). Cluster analysis based on unweighted-pair group method with arithmetic averages (UPGMA) and Jaccard distance was used for grouping samples. Distances in the dendrogram are scaled by Wishart's objective function (E), which is a measure of information loss as agglomeration proceeds and is equal to the sum of square of the errors from each centroid to the items in that group (McCune and Grace 2002). The percentage of information remaining can be expressed as $100(\text{TSS}-E)/\text{TSS}$, where TSS is the total sum of squared deviations from the centroid when all items are fused into one group. Therefore, the information remaining is conceptually similar to an r^2 value (fraction of variance explained by a regression).

Canonical correspondence analysis (CCA) is designed to extract synthetic environmental gradients from ecological data sets (McCune and Grace 2002). This technique assumes unimodal distribution of species abundance along an environmental gradient, which commonly occurs in most ecological data sets. We used CCA to elucidate the relationships between bacterial community structure and environmental variables, including chemoautotrophic production, prokaryotic abundance, O_2 , H_2S , $\text{S}_2\text{O}_3^{2-}$, H_4SiO_4 , NO_3^- , PO_4^{3-} , SO_3^{2-} , NH_4^+ , and NO_2^- . We realize the potential importance of surface chlorophyll α concentration and primary production (PP) in affecting bacterial population dynamics in the basin's interior. However, depths of surface phytoplankton measurements do not correspond to those of T-RFLP samples and cannot be incorporated into canonical correspondence analyses directly. Therefore, organic carbon (generally reflecting surface PP) and terrigenous material flux into sediment traps were used for interpretation of our observations. Terrigenous material flux is estimated as terrigenous flux = total mass flux – silica flux – inorganic carbon flux – (carbon flux \times 2.5) (R. Thunell, pers. comm.). Based on relative abundance of terminal restriction fragments (T-RFs), we attempted to find distribution patterns of bacterial populations within redox gradients, and to understand which biogeochemical parameters contributed to variations among stations. Biplots were generated to show the relationship between environmental variables and each dimension from the CCA analysis. The angle and length of the vector indicate the direction and strength of the relationship (McCune and Grace 2002).

Generally, a single ordination technique cannot uncover both "species composition representation" (like nonmetric multidimensional scaling [NMS]) and "gradient analysis" (like CCA) (De'ath 1999). When species composition is controlled by external factors, such as disturbances by terrestrial input and oxygen intrusions, rather than by internal factors or environmental gradients, NMS would be a better a priori choice. NMS is an ordination method maximizing rank-order correlation between the original data set and ordination space based upon an iterative optimization procedure. In PC-ORD, we chose the

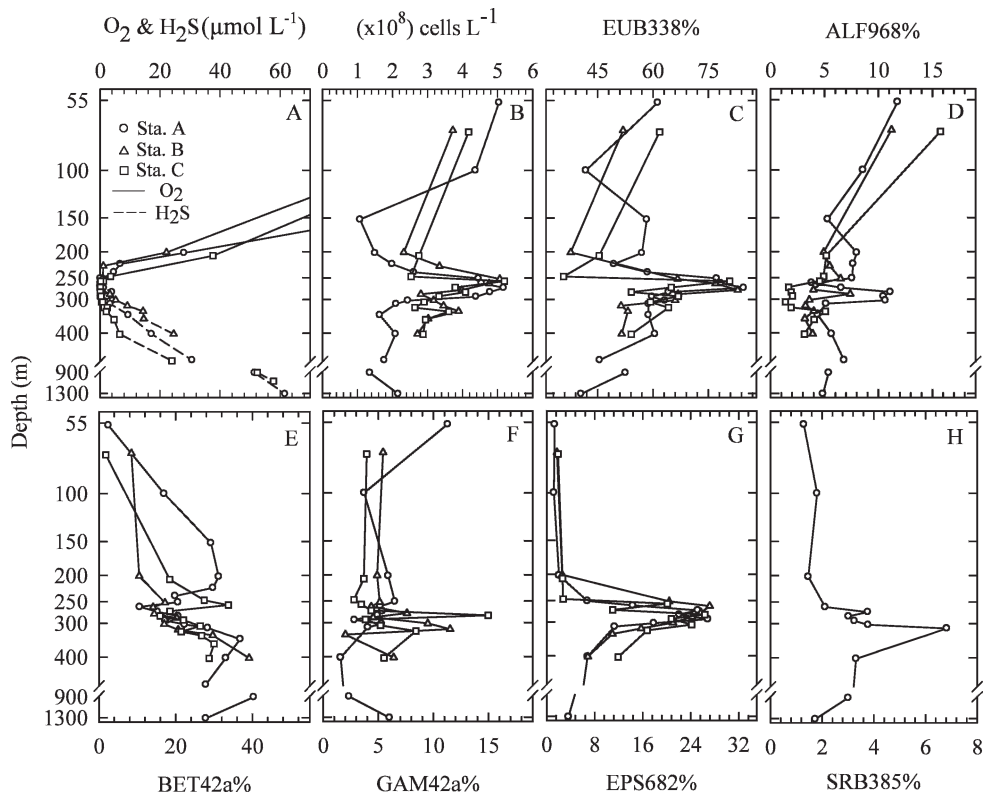


Fig. 2. Three-station comparison of vertical profiles of (A) O_2 and H_2S , (B) abundance of prokaryotic cells, and (C–H) relative abundances of different phylogenetic groups of bacteria determined by FISH: (C) eubacteria, (D) α -proteobacteria, (E) β -proteobacteria, (F) γ -proteobacteria, (G) ϵ -proteobacteria, and (H) sulfate reducers belonging to δ -proteobacteria.

autopilot run with the slow and thorough option, which produces a solution by choosing the axis that minimizes stress and maximizes the interpretation of the data as assessed by the amount of variability explained in the data set (McCune and Grace 2002). Stress is an indicator of goodness of fit because it measures the inverse of the fit between the original data matrix and the reduced-dimension ordination matrices. Stress values less than 15 indicate that data are well-represented in multivariate space and risks of drawing false inferences are low. Monte Carlo tests were used to identify dimensions with solutions that were significantly different than those due to random chance. The relationship between environmental variables and ordination scores from the NMS analysis is shown with a joint plot. Similarly, the angle and length of the vector in this joint plot indicate the direction and strength of the relationship.

Pearson product moment correlation analyses were carried out with SigmaStat 3.10 software (Systat Software) to test relationships among absolute abundances of different phylogenetic bacterial groups, mean OTU richness, chemoautotrophic production in the redoxcline, and surface primary production.

Results

Spatial variations in bacterial community composition—FISH measurements: Previous studies in the Cariaco

Basin's water column have revealed vertical zonation in the chemical environment that is largely independent of water-density structure (Taylor et al. 2001; Ho et al. 2004). Figure 2 shows biotic and abiotic characteristics of the water column during the CAR-112 cruise, representing typical microbial profiles in the Cariaco system. Oxygen concentrations dramatically decrease below the euphotic zone and usually reach undetectable levels below 250 m (Fig. 2A). Below this depth, sulfide increases to a maximum of $62 \mu\text{mol L}^{-1}$ at 1,300 m near the bottom of the basin (Fig. 2A).

Bacterial community structure assessed by FISH clearly illustrated varying bacterial community composition as a function of depth. Among the three stations, total prokaryotic abundance varied from 1.1×10^8 to 5.2×10^8 cells L^{-1} (Fig. 2B). Consistently, prokaryotic abundances peaked in surface waters, containing 5.0×10^8 , 3.7×10^8 , and 4.2×10^8 cells L^{-1} at Stas. A, B, and C, respectively. Total abundances decreased to minima around 200 m, averaging $2.1 \pm 0.5 \times 10^8$ cells L^{-1} , and then increased to midwater maxima at the O_2/H_2S interface, where cell abundances of about 5.2×10^8 cells L^{-1} were found at all three stations. Stas. B and C, but not A, had a third abundance peak at 330 m, with values of 3.9×10^8 cells L^{-1} at Sta. B and 3.6×10^8 cells L^{-1} at Sta. C. Below 400 m at Sta. A, prokaryotic abundances remained relatively constant ($1.8 \pm 0.4 \times 10^8$ cells L^{-1}) down to the bottom of the basin (1,400 m). The EUB338 probe detected

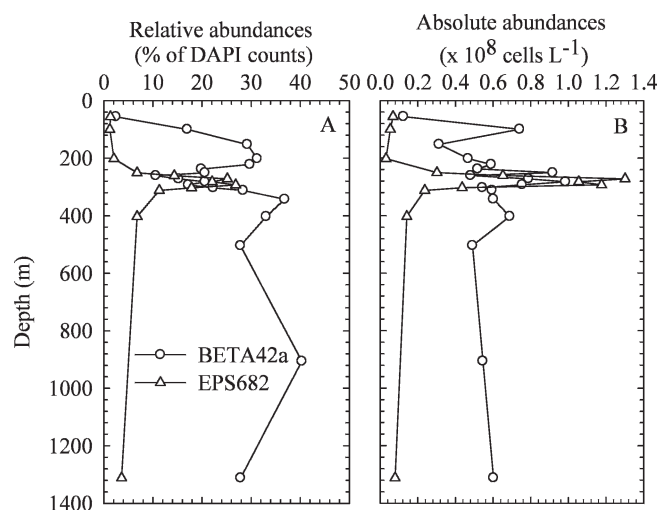


Fig. 3. Vertical profiles of β - and ϵ -proteobacteria plotted as both (A) relative and (B) absolute abundances reveal different features in their vertical distribution.

the highest proportions of total prokaryotes near the oxic-anoxic interface, with relative abundances of 85%, 83%, and 81% at Stas. A, B, and C, respectively (Fig. 2C). The proportion of EUB338-positive cells relative to DAPI-stained cells did not significantly differ among stations and was on average $53\% \pm 5\%$ in the oxic zones, $65\% \pm 2\%$ in the redoxclines, and $46\% \pm 6\%$ in the anoxic zones at all stations.

Alpha-proteobacteria (ALF968-positive cells) were most abundant in surface waters, reaching 12% of DAPI counts at Stas. A and B, and 16% at Sta. C (Fig. 2D). Throughout the water column, α -proteobacteria represented only a minor fraction of total prokaryotic inventories, averaging $5\% \pm 2\%$, although at Sta. A, the redoxcline supported a small peak of α -proteobacteria (10%).

The β -proteobacteria (BET42a-positive cells) in surface waters of all stations accounted for a minor fraction of DAPI counts (2% at Stas. A and C, 8% at Sta. B), and they increased from 15% at the interface to as high as 40% at 400 m, then remained relatively constant ($\sim 30\%$) below 400 m (at Sta. A) (Fig. 2E). The three β -proteobacterial profiles differed at a depth of about 200 m, with increasing relative abundances from Sta. B (10%) to C (18%) and A (31%). The disparity in β -proteobacterial proportions at this depth suggests the likely role of significant differences in environmental variables between the two basins and near the sill. However, relative abundances of β -proteobacteria below 250 m remained similar among stations. No BETA2-870-positive cells (β -proteobacteria) were detected throughout the water column, suggesting that β -proteobacteria in the Cariaco Basin were phylogenetically different from those in most freshwater systems.

At Sta. A, γ -proteobacteria (GAM42a-positive cells) had their highest relative abundance in surface waters and dramatically decreased below 100 m, reaching on average 4.5% of DAPI counts throughout the rest of the water column (Fig. 2F). In contrast, γ -proteobacteria peaked ($11\% \pm 3\%$) near the interfaces of Stas. B and C, and decreased to about 4% of DAPI counts averaged over the rest of depths (Fig. 2F).

Both sulfate-reducing δ -proteobacteria (SRB385-positive cells) and ϵ -proteobacteria (EPS682-positive cells) were almost undetectable ($<2\%$) above 200 m (Fig. 2G,H). Sulfate reducers peaked at 310 m and decreased below 400 m (Fig. 2H). In contrast, ϵ -proteobacteria consistently increased to maxima ($\sim 27\%$) near the interface at all three stations and then dramatically declined to 4% of the prokaryotic inventory below 400 m at Sta. A (Fig. 2G). Interestingly, ϵ -proteobacterial peaks in relative abundances corresponded with depths of depressed β -proteobacterial relative abundances (Fig. 3A). In contrast, absolute abundances of β -proteobacteria increased with

Table 1. Summary of bacterial OTU richness observed from six cruises. The first column presents approximate depths, deviating about ± 5 m from true depths. “—” indicates DNA samples not collected from this depth.

Depth (m)	CAR112-A (May 05)	CAR112-B (May 05)	CAR112-C (May 05)	CAR-108 (Jan 05)	CAR-100 (May 04)	CAR-96 (Jan 04)
Surface (20–60 m)	35	35	34	38	38	—
150	28	—	—	—	—	—
200	—	32	35	—	—	—
235	23	—	—	—	—	—
250	31	35	37	36	—	—
260	33	—	—	—	—	—
270	29	38	37	34	36	23
280	28	—	38	35	—	22
290	31	—	32	35	39	—
300	27	36	—	28	—	—
310	—	—	38	38	36	—
320	—	35	38	37	—	32
350	—	38	—	40	—	—
400	31	30	38	—	—	—
500	29	—	—	30	—	—
1300	31	—	—	—	31	29
Average \pm SD	29.6 \pm 3.1	34.9 \pm 2.7	36.3 \pm 2.2	35.1 \pm 3.7	34.8 \pm 3.3	26.5 \pm 4.8
Total unique OTUs	78	74	83	75	68	52

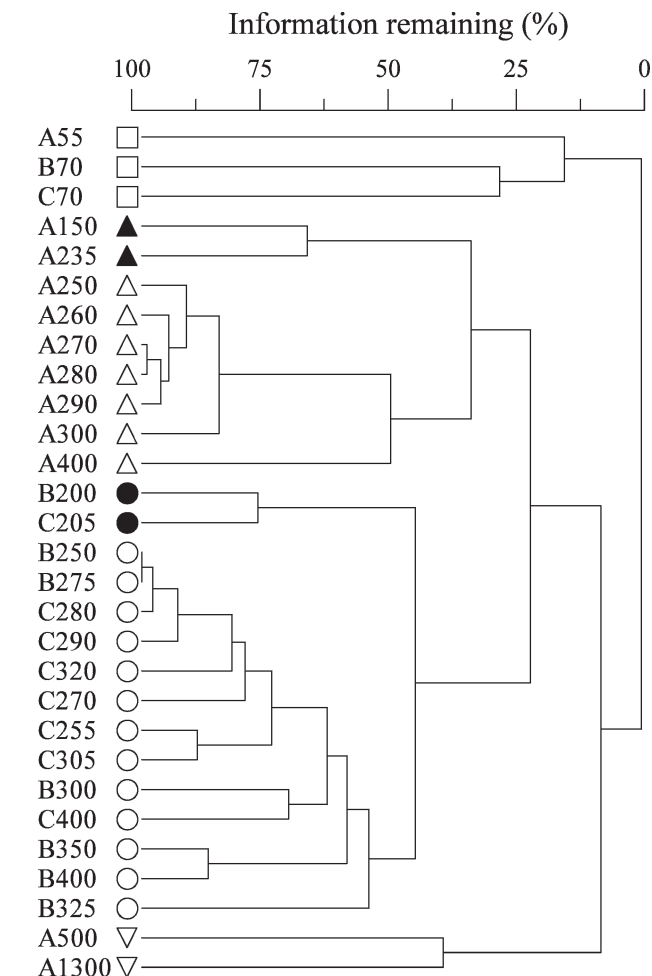


Fig. 4. Cluster analysis of T-RFLP patterns using UPGMA method and Jaccard distance as a measure of similarities in OTU composition among samples. Letters “A, B, C” represent Stas. A, B, and C. The number and symbols following “A, B, C” indicate sample depths and groups formed by partitioning the dendrogram, respectively. Information remaining is conceptually similar to an r -squared value (see Methods).

depth; one peak occurred at 100 m, and one peak occurred within the redoxcline. The inverse correlation between relative abundances of β - and ϵ -proteobacteria in the redoxcline was not evident from the plot of their absolute abundances (Fig. 3B).

T-RFLP assessments—Mean OTU richness for discrete depths at Sta. A (30 ± 3) was significantly lower (t -test, $n = 9$, $p < 0.005$) than that at Stas. B (35 ± 3) and C (36 ± 2) (Table 1). The total number of unique OTUs present at Stas. A, B, and C was 78, 74, and 83, respectively (Table 1). Cluster analysis of T-RFLP patterns demonstrated that bacterial assemblages differed greatly among sites and depths (Fig. 4). For example, OTU compositions in surface samples from the three stations were only 30% similar at most, while samples within Sta. A’s redoxcline had OTU compositions that were very different from the 55-m sample, but were about 80% similar to one another.

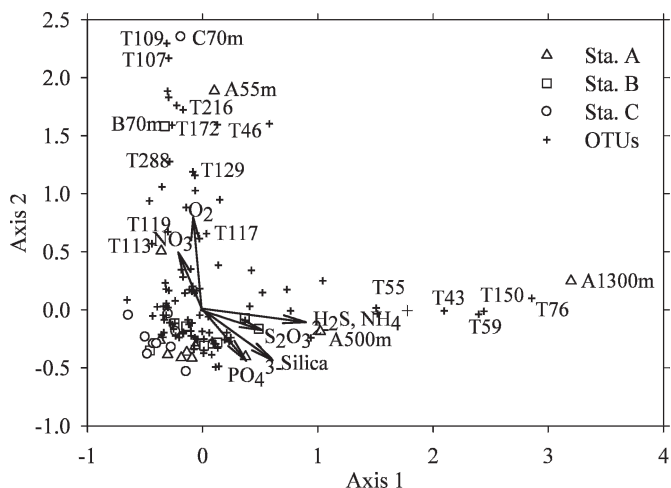


Fig. 5. A biplot generated from the CCA of T-RFLP profiles of CAR-112 samples at Stas. A, B, and C. Environmental variables are represented by arrows, with cutoff of $r^2 = 0.2$. Eigenvalues (400 runs) were 0.326 and 0.178 for axes one and two, respectively. Labeled OTUs with fragment size (e.g., T109) are unique in oxic or anoxic samples. Most OTUs are not labeled for the sake of clarity.

Based on dendrogram topology (Fig. 4), we divided samples into six groups: (1) bacterial communities in surface waters (A55, B70, C70) that showed low similarity among sites and with other depths; (2) and (3) bacterial communities from oxic/suboxic depths in the aphotic zone that differed from other depths and among stations (A150, A235, B200, C205); (4) and (5) T-RFLP patterns in the redoxcline of Sta. A (A250, A260, A270, A280, A290, A300, A400) were grouped together, but separated from those in Sta. B (B250, B300, B325, B350, B400) and C (C255, C270, C280, C290, C305, C320, C400); and (6) bacterial assemblages in the deep anoxic waters (A500 and A1300) were quite different from those found in overlying waters. Overall, variations in bacterial community structure within redoxclines alone were greater on horizontal (Stas. B and C versus A) than on vertical (within redoxclines) scales, while variations among oxic, redoxcline, and anoxic zones were greater on vertical than on horizontal scales.

Canonical correspondence analyses of T-RFLP patterns related to environmental gradients during the CAR-112 cruise—Canonical correspondence analyses organized the T-RFLP profiles representing community compositions from different depths and stations along environmental gradients (Fig. 5). This two-dimensional plot showed that the first and second axes explained 17.5% and 10.9% of the total variance among T-RFLP profiles, respectively (Monte Carlo test of Eigenvalue, $p \leq 0.005$). T-RFLP profiles were mainly separated along two vectors representing O_2 and H_2S gradients. The O_2 and NO_3^- vectors defined the oxic to suboxic environmental gradient, and several unique OTUs were separated from the total OTU pool, such as 46, 107, 109, 172 bp in surface waters and 113, 117, 119, 129 bp in the nitrification zones (150–235 m). Meanwhile, H_2S , PO_4^{3-} , SO_3^{2-} , NH_4^+ , and H_4SiO_4 vectors pointed to

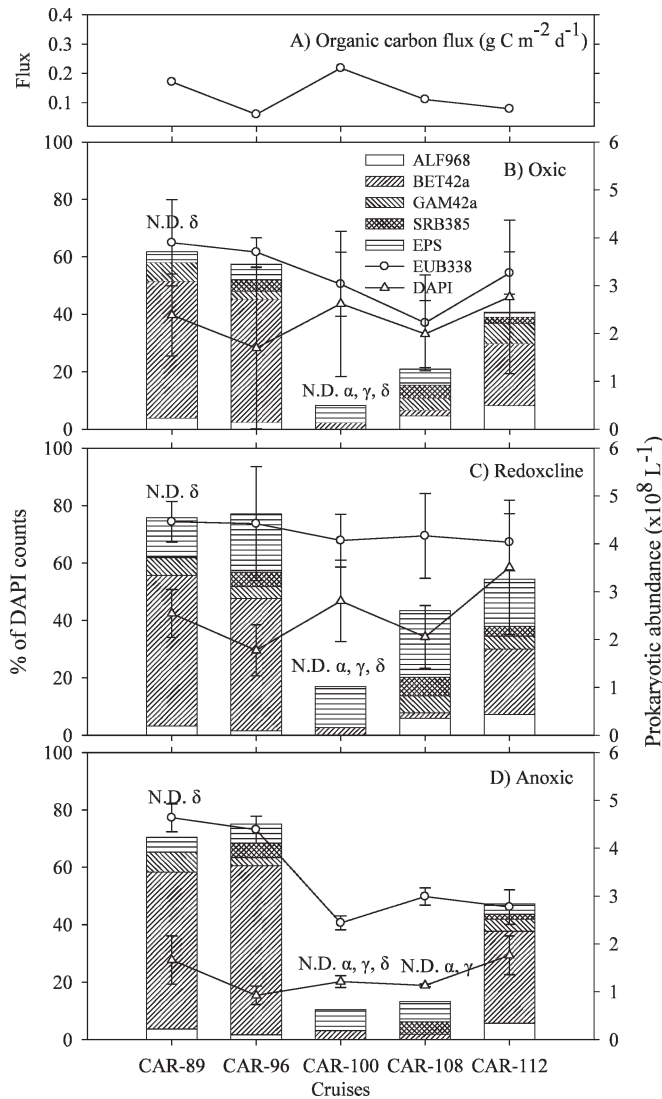


Fig. 6. (A) Temporal variations in organic carbon flux ($\text{g C m}^{-2} \text{d}^{-1}$) at 225 m, averaged values for prokaryotic abundances, and relative abundances of specific bacterial groups in (B) oxic, (C) redoxcline, and (D) anoxic zones. Error bars are standard deviations. Symbols (α , γ , or δ) above bars indicate that these subdivisions of proteobacteria were not determined (N.D.) during those cruises.

a cluster of samples below 400 m, and separation of specific OTUs, such as 43, 55, 59, 76, and 150 bp. Some variables (NO_2^- , SO_3^{2-} , chemoautotrophic and heterotrophic production) do not appear in the graph due to the threshold setting of $r^2 = 0.2$, suggesting that coupling between these variables and general distribution patterns of bacterial assemblages was weak. Most OTUs were centralized near the cross point of the two axes, suggesting that these OTUs were not organized by the suite of measured environmental variables.

Temporal variations in environmental conditions and bacterial assemblages at Sta. A—Temporal variations in bacterial populations at the time-series Sta. A were compared based on averaged values of relative abundances

within oxic, redoxcline, and anoxic zones (Fig. 6). Within the 2 yr surveyed, prokaryotic abundances varied with seasonal shifts of organic carbon flux captured in sediment traps, showing $\sim 45\%$ higher abundances in May than in January in oxic waters and the redoxcline. However, seasonal trends of prokaryotic abundances in deep anoxic waters were not consistent with those in overlying waters, and prokaryotic abundances were $\sim 57\%$ higher in CAR-89 and 112 cruises than in CAR-96, 100, and 108 cruises. Proportions of DAPI counts detected by the EUB338 probe in the oxic zone varied roughly with contributions of β -proteobacteria instead of total prokaryotic abundances. The covariation between relative abundances of EUB338- and BET42a-positive cells was less evident in both the redoxcline and anoxic zones. Within the redoxcline, contributions of EUB338-positive cells only varied by $\sim 5\%$ over the 2 yr, while β -proteobacteria showed wide temporal variations in this zone. The temporal shift in relative abundances of BET42a-positive cells showed that β -proteobacteria dominated ($50\% \pm 6\%$) prokaryotic inventories during CAR-89 and 96 cruises, decreased to $3\% \pm 0.6\%$ in CAR-100 and 108 cruises, and again increased to $25\% \pm 6\%$ in the CAR-112 cruise. Temporal variations in $\Delta\rho$ and relative abundances of β -proteobacteria were not consistent (Fig. 7); there was a relatively high $\Delta\rho$ value (meaning strong lateral intrusions of Caribbean midwater masses) during the CAR-100 cruise and near-zero values of $\Delta\rho$ in the CAR-89, 96, 108, and 112 cruises.

Epsilon-proteobacterial proportions remained relatively constant between cruises, averaging $4\% \pm 2\%$ of DAPI counts in the oxic zone, $18\% \pm 4\%$ in the redoxcline, and $6\% \pm 2\%$ in the deep anoxic waters. Similarly, α - and γ -proteobacteria, and sulfate-reducing bacteria belonging to δ -proteobacteria on average contributed $4\% \pm 2\%$, $5\% \pm 2\%$, and $4\% \pm 2\%$ to prokaryotic inventories in the three layers throughout the cruises surveyed.

Bacterial T-RFLP patterns showed that mean OTU richness within discrete samples varied among cruises (Table 1). At the time-series station, the CAR-100 and 108 cruises had relatively high OTU richness, averaging 36 ± 3 on both dates. In contrast, the CAR-96 cruise had the lowest OTU richness (26 ± 5), and the CAR-112 cruise had an intermediate value of 30 ± 3 . Nonmetric multidimensional scaling analysis of T-RFLP patterns revealed significant temporal shifts in bacterial community composition within the redoxcline during the four cruises at Sta. A (Fig. 8). After 36 iterations, the stress of the final solution was 11.2 (below the benchmark of 15) and therefore considered stable (Table 2). The final solution showed that two axes explained 84% of the cumulative variance in the data set. The resulting graphs in two-dimensional space demonstrated that T-RFLP patterns in the CAR-100 and CAR-108 cruises grouped together (Fig. 8). Meanwhile, they were well separated from bacterial communities in the CAR-96 cruise along axis two. In addition, bacterial community compositions formed two clearly separated clusters along axis one. This multivariate statistical analysis of T-RFLP patterns correlated well with temporal changes in bacterial populations assessed by the FISH technique, which showed significant variations between cruises,

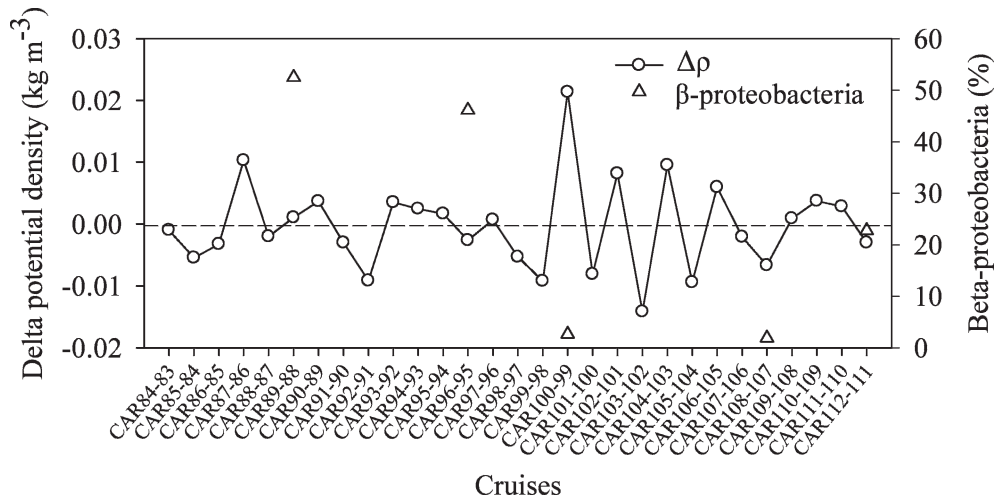


Fig. 7. Temporal variations in delta potential densities ($\Delta\rho$) and relative abundances of β -proteobacteria within the redoxline at Sta. A. Both values are averaged within the redoxline (250–400 m). Horizontal line indicates zero values of $\Delta\rho$.

especially in β -proteobacteria populations. Additionally, NMS ordination revealed the appearance of OTUs unique to each sampling date (Fig. 8).

A correlation analysis was performed to get an overview of the relationships among FISH-generated bacterial abundances, diversity (OTU richness), and functions (chemoautotrophic production and surface primary production) in the redoxline. We restricted this analysis to data from four cruises at three stations, except that there were no data for surface primary production at Stas. B and C. Table 3 shows that OTU richness (T-RFLP-derived) was negatively correlated with β -proteobacterial abundances (FISH-derived) and positively but weakly correlated with other measurements (e.g., prokaryotic abundances

and chemoautotrophic production). Meanwhile, chemoautotrophic production was better correlated with abundances of γ - and ϵ -proteobacteria, suggesting these two groups may contribute to a significant portion of dark CO_2 fixation in the redoxline. Interestingly, β -proteobacterial abundances were inversely correlated with surface primary production. The ecological implication behind this inverse correlation is unclear and awaits further investigation.

To explore relationships between bacterial T-RFLP profiles and environmental variables, we selected measurements consistently determined for all four cruises, including prokaryotic abundance, O_2 , H_2S , PO_4^{3-} , NH_4^+ , and H_4SiO_4 , NO_2^- , and chemoautotrophic production. These factors are not necessarily the most important forces controlling bacterial population dynamics, but they can be used to infer relationships to important biogeochemical processes. Among all biogeochemical parameters for generating a joint plot, only prokaryotic abundance, PO_4^{3-} , and NO_3^- were correlated ($r^2 > 0.2$) with temporal separation of samples. Samples from the CAR-112 cruise had relatively high bacterial abundances compared with samples from other cruises. Water properties associated with bacterial T-RFLP patterns in the CAR-100 and CAR-108 cruises were characterized by high PO_4^{3-} concentrations. Interestingly, the separation of the CAR-108 250-m sample from other samples corresponded well with an unusually high concentration of NO_3^- at this depth, indicating either oxygen intrusion or deepening of the redoxline prior to our sampling time. Weak correlations ($r^2 < 0.2$) between bacterial T-RFLP patterns and other variables indicated a low dependence of diversity patterns on most measured variables.

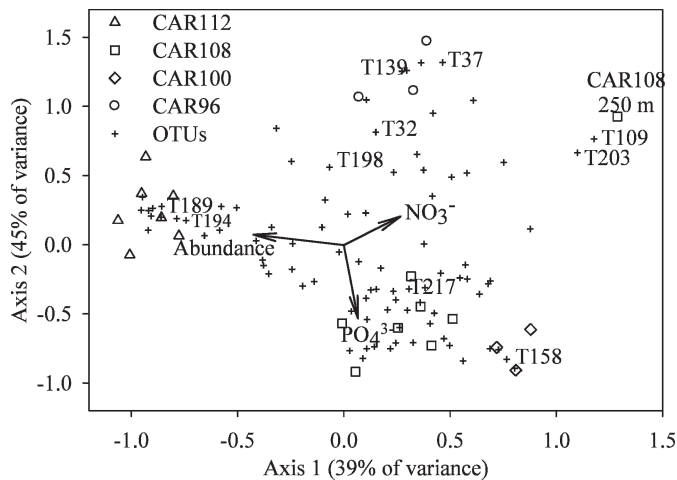


Fig. 8. NMS ordination of temporal T-RFLP patterns for redoxline samples taken during cruises CAR-96, CAR-100, CAR-108, and CAR-112. Values in parentheses of each axis title indicate percentage of variance explained by this axis. Plus symbols represent unique OTUs. OTUs dominating or unique in each cruise are labeled with fragment size (e.g., T139).

Discussion

Bacterial distribution patterns responding to redox gradients—Complexity in environmental conditions can vary on multiple spatial scales and is likely to influence bacterial

Table 2. Stress in relation to number of axes, showing that relationships between extracted axes and real data are stronger ($p < 0.05$) than expected by chance alone as determined by a Monte Carlo randomization test.

Axis	Stress in real data, 40 runs			Stress in randomized data, 50 runs			p
	Minimum	Mean	Maximum	Minimum	Mean	Maximum	
1	30.16	43.59	54.88	35.10	48.85	54.77	0.02
2	11.18	14.44	31.43	18.88	23.45	35.65	0.02

diversity (Loreau 1998; Konopka 2006). Vertical stratification of geochemical variables is prominent in the Cariaco water column and potentially allows for differentiation of bacterial assemblages along the redox gradient (Taylor et al. 2001, 2006; Ho et al. 2004). Waters between the base of the photic zone and 250 m are characterized by high nitrate and diminishing concentrations of oxygen, whereas the redoxcline (250–400 m) exhibits undetectable concentrations of oxygen and active cycling of inorganic redox couples either abiotically or biotically. Below 400 m, sulfate reduction is likely to occur at significant rates, with sulfide concentration increasing to the bottom of the basin.

Patterns in bacterial distribution along the gradient were visualized by FISH profiles (Fig. 2), cluster analysis (Fig. 4), and CCA (Fig. 5) of T-RFLP profiles. These patterns are consistent with the hypothesis that zonation of electron donors and acceptors organizes the array of bacterial assemblages residing here. FISH profiles in this study showed depth-dependent variations of specific bacterial populations. Similarly, canonical correspondence analyses of bacterial community composition revealed that unique OTUs were prevalent under different redox conditions (Fig. 5). However, some OTUs did not seem to separate along redox gradients, indicating that these organisms may tolerate a wide range of oxygen and sulfide concentrations or that 16S rRNA sequence variability does not necessarily reflect functional diversity (Ward 2005). Unfortunately, lack of sequencing data made the phylogenetic assignment of OTUs difficult and subsequently limited our understanding of OTU diversity and ecological analysis.

Factors affecting among-site differences of bacterial community structure—Generally, bacterial community composition is responsive to water properties and varying scales of disturbance (Buckling et al. 2000; Konopka 2006).

One interesting finding of our cluster analysis of T-RFLP patterns (Fig. 4) is that variations in bacterial community structure in the redoxcline were greater among sites (Stas. B and C versus A) than over vertical (within the redoxcline) scales, possibly due to higher horizontal variation in biotic (surface primary production, organic flux, grazing pressure) and abiotic (fluvial discharge, oxygen intrusion, alternative oxidants) variables. In the Cariaco system, the western basin usually has lower surface primary production than the eastern basin (Richards 1975; Scranton et al. 1987; Muller-Karger et al. 2001), which may to some degree explain the differences in bacterial community structure between Sta. A and Sta. C. Sta. B is closer to Sta. A than C, and it is located in the path of potential water intrusions from the Caribbean Sea through the Canal de la Tortuga, which can experience disturbances driven by mesoscale eddy migrations (Astor et al. 2003).

Several subtle differences in bacterial community composition between sites may provide hints about forces driving disparities. In Fig. 2, differences between stations were most evident around 200 m, where the occurrence of oxygen intrusions has been observed (Scranton et al. 2001). Within the depth range of 150 to 235 m, proportions of EUB338- and BET42a-positive cells at Stas. B and C were much lower than at Sta. A. Consistently, B200 and C205 samples formed one independent group in the cluster analysis of bacterial communities (Fig. 4). Based on geological and physical characteristics of the Cariaco system (Fig. 1), Stas. B and C are closer to channels and more susceptible to disturbance due to oxygen intrusion compared to Sta. A. In addition, Stas. B and C had broader suboxic zones than Sta. A during the CAR-112 cruise, suggesting that lateral intrusions of oxic waters likely had more significant effects on water properties in Stas. B and C than Sta. A (Percy et al. in press). Although obvious increases in O_2 concentration were not observed in the

Table 3. Pearson product moment correlation analyses among absolute abundances of different phylogenetic bacterial groups, mean OTU richness, chemoautotrophic productions averaged within the redoxcline, and surface primary production.

Measurements	OTU richness		Chemoautotrophic production		Surface primary production	
	r	p	r	p	r	p
Prokaryotic abundance	0.46	0.356	0.61	0.205	−0.25	0.751
Eubacteria	0.40	0.432	0.54	0.268	−0.28	0.717
α -proteobacteria	0.14	0.797	0.32	0.531	−0.52	0.485
β -proteobacteria	−0.40	0.427	0.48	0.331	−0.88	0.116
γ -proteobacteria	0.69	0.131	0.83	0.041	0.05	0.951
ϵ -proteobacteria	0.51	0.298	0.92	0.009	−0.52	0.482
OTU richness	–	–	0.48	0.337	0.74	0.265
Chemoautotrophic production	–	–	–	–	−0.52	0.480

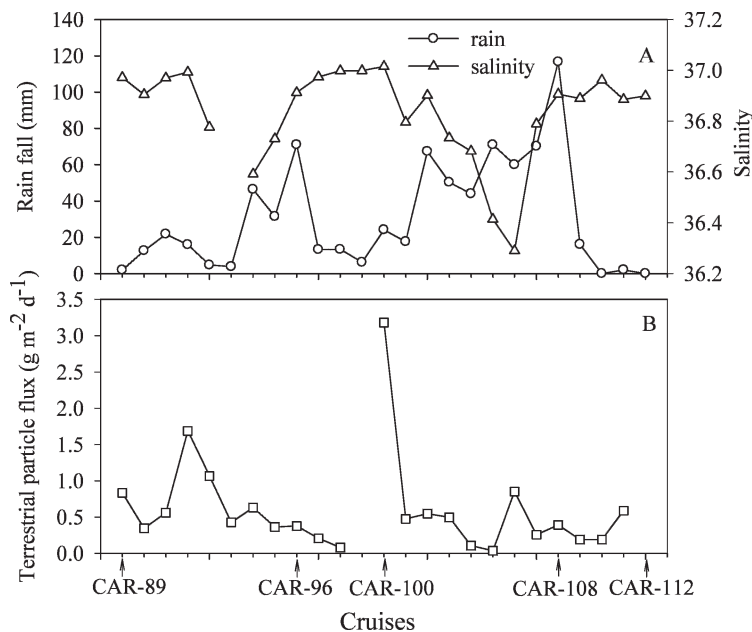


Fig. 9. (A) Temporal variations in rainfall (recorded at Punta de Piedras Sta.), surface salinity, and (B) terrigenous material flux to 225 m at the Cariaco time-series station. Terrigenous material flux was estimated indirectly as total mass flux – silica flux – inorganic carbon flux – (carbon flux \times 2.5).

oxygen sensor data in this depth range, oxygen intrusions have occasionally been detected during previous Cariaco cruises (Scranton et al. 2001). Additionally, laterally transported water masses do not necessarily have an oxygen signature if microbial respiration, or chemical reactions have consumed residual oxygen prior to sampling time. The products of oxygen removal processes may serve as electron acceptors for members of the microbial community.

In terms of energy and nutrient gradients, the redoxcline is to some degree similar to open ocean deep chlorophyll maxima (DCM), and it is sensitive to subtle changes in physical and chemical conditions (Oguz et al. 2001; Huisman et al. 2006). Just like DCM oscillations and chaos induced by intermittent mixing, oxygen intrusions may influence kinetics of the “Fe and Mn shuttles” in the redoxcline and subsequently enhance availability of specific oxidants at depth and lead to significant community shifts (Davison et al. 1982; Ho et al. 2004; Huisman et al. 2006). Although we can not exclude the influence of various stochastic events (e.g., movement of the redoxcline and terrestrial input) leading to the observed patterns, it is likely that lateral intrusions of oxic water from outside of the basin influence among-site variations in bacterial community composition.

Internal and external forcing of temporal dynamics in bacterial assemblages—Knowledge of environmental context is essential for investigating the mechanisms that drive bacterial distribution and diversity. Microbial population dynamics are generally consequences of several factors, including the spatiotemporal heterogeneity in the physico-chemical “landscape,” rapid physiological acclimation of

microbes to environmental variations, trophic interactions between different microbes (predation by bacterivores and viral lysis), and the capacity for rapid genetic changes (Konopka 2006).

The present study clearly shows temporal variations of bacterial populations over 2 yr at the CARIACO time-series stations. Correlation analyses do not reveal significant relationships between diversity (OTUs) and functions (chemoautotrophic production and surface primary production), although temporal variations in chemoautotrophic production were strongly related to abundances of γ - and ϵ -proteobacteria. Both FISH and T-RFLP analyses reveal that bacterial community compositions during the CAR-100 and 108 cruises were distinct from the other three cruises (Figs. 6, 8). The two cruises (CAR-96 and 112) in which β -proteobacteria (FISH-derived) were most common had lower OTU richness (T-RFLP-derived) than the two other cruises (CAR-100 and 108), which exhibited lower β -proteobacterial abundances. Why β -proteobacteria exhibited such remarkable temporal variations while other groups of bacteria remained relatively unchanged is puzzling. Our current data are insufficient to confidently infer functional roles of β -proteobacteria in the Cariaco water column. Since β -proteobacteria are commonly typified as dominating freshwater systems and as almost nonexistent in marine environments (Nold and Zwart 1998), abundant β -proteobacteria in the Cariaco Basin could be due to terrestrial input from surrounding rivers and surface runoff. However, application of the probe BETA2-870 (which targets a cosmopolitan freshwater lineage of β -proteobacteria) did not detect β -proteobacteria in the Cariaco samples, suggesting that river runoff may not be the only dominant source of β -proteobacterial

biomass in the Cariaco Basin. Furthermore, no apparent relationship exists between temporal variations in β -proteobacterial abundance and amount of rainfall recorded at the Punta de Piedras meteorological station northeast of the Cariaco Basin (Figs. 6, 9A). For example, rainfall in Jan 05 alone (CAR-108) was four times the annual average for the previous 10 yr, and yet β -proteobacteria were almost undetectable during this cruise. Rainfall recorded at the Cumana and Caracas meteorological stations was consistent with values recorded at the Punta de Piedras station (L. Lorenzoni, pers. comm.), suggesting that freshwater input from continental runoff to the Cariaco Basin would likely be nearly synchronous with local rainfall.

Generally, contributions of small rivers along the Venezuelan coastline to the basin's nutrient budget are believed to be of limited significance (F. Muller-Karger, unpubl. data). However, sediment transport can be important. Unusually large amounts of terrigenous material flux were captured in the sediment trap below 225 m prior to the CAR-100 cruise, when β -proteobacteria were close to undetectable levels (Figs. 6, 9B), suggesting that episodic events like terrestrial inputs may significantly change biogeochemical processes in the water column and subsequently lead to shifts in bacterial community composition. The two cruises with depressed β -proteobacterial abundance were characterized by either high terrigenous flux (CAR-100) or high rainfall (CAR-108). Furthermore, both surface salinity and β -proteobacterial abundances were low in surface waters when β -proteobacteria were prevalent in the rest of the water column. Considering all available information, it appears unlikely that river runoff is the primary source of β -proteobacteria.

Since β -proteobacteria in the Cariaco Basin were readily detected by the probe BET42a and were undetectable by the probe BETA2-870, β -proteobacteria may be phylogenetically divergent from freshwater β -proteobacteria and potentially be locally active. Within the Cariaco oxic-anoxic transition zone, RubisCO genes from *Thiobacillus denitrificans* were found (A. Chistoserdov, pers. comm.), suggesting that some β -proteobacteria may be involved in sulfur and nitrogen cycling. On the other hand, the anoxic Cariaco Basin is rich in methane and is characterized by high methane oxidation rates below the redoxcline (Ward et al. 1987; Kessler et al. 2005), which is quite consistent with distributions of β -proteobacteria (Fig. 3). FISH combined with microautoradiography demonstrated that β -proteobacteria in the redoxcline were unable to assimilate ^3H -leucine (Lin et al. 2007), indicating that they may have C-1 metabolism, be chemolithoautotrophs, or simply lack leucine transporters. It is well-known that some members of β -proteobacteria are methylotrophic (Hanson and Hanson 1996). Our preliminary data show that several cloned sequences from the Cariaco anoxic waters are affiliated with *Burkholderia* (X. Lin, unpubl. data). Recently, methylotrophy modules have been found in genomes of *Burkholderia xenovorans* (Chistoserdova et al. 2005), suggesting that some β -proteobacteria may have methanotrophic or methylotrophic activities in the Cariaco

Basin. Therefore, it is likely that β -proteobacteria throughout the Cariaco water column may be functionally differentiated depending on chemical zonation.

Although both FISH results and NMS ordination of T-RFLP patterns show clear temporal changes of bacterial populations at the time-series stations, shifts in bacterial community structure were not correlated with measured environmental variables. This suggests that distribution patterns of bacterial assemblages may be driven by other internal (e.g., positive or negative interactions) or external (e.g., disturbance) factors. For example, Lin et al. (2007) demonstrated that bacterivorous predation could significantly alter bacterial community composition in the redoxcline of the Cariaco Basin, further complicating the underlying forces that drive the dynamics of bacterial community composition. In addition, differences in potential density ($\Delta\rho$) among neighboring months at Sta. A (Fig. 7) indicated that the CAR-100 cruise, with low proportions of β -proteobacteria, was characterized by a high $\Delta\rho$ value, suggesting that disturbance by lateral intrusions of Caribbean midwater masses may have dramatic impacts on bacterial population dynamics within the basin. However, low proportions of β -proteobacteria were observed during CAR-108, when $\Delta\rho$ values were low, and, conversely, other cruises with low $\Delta\rho$ values exhibited high β -proteobacteria abundances (Fig. 7). Alternatively, our understanding of bacterial population dynamics is further confounded by low sampling frequencies. Based on varying sampling frequency (hours to seasons) in the NW Mediterranean Sea, Ghiglione et al. (2005) argued that long-term studies should involve a minimum sampling timescale of 2 weeks. Without knowing the preceding history of a community (ranging from minutes to weeks), it is difficult to infer cause and effect. For example, we occasionally observed vertical mismatches between thiosulfate/sulfite inventories and putative sulfur-fueled chemoautotrophic production (or biomass) peaks, suggesting a succession of events from substrate accumulation to its depletion with attendant biomass increases (Hayes et al. 2006). In a recent review paper, Ward (2005) noted that the presence of large populations of certain microbes at one point in time does not necessarily imply that the coexisting environmental conditions are favorable for that organism. Therefore, the history of a community can matter more than the instantaneous environmental conditions, and spatial and temporal mismatches between environmental variables and bacterial populations may bias our understanding of response patterns.

The present study has demonstrated, with the aid of multivariate statistical tools, that there are clear spatio-temporal variations in bacterial community composition. These variations were related to spatial heterogeneity of geochemical properties, and most likely terrestrial input as well as lateral intrusions of adjacent waters. The redox state seems to be an important driving force for separation of unique OTUs through anoxic water columns, while among-site variations in bacterial community structure may be ascribed to differences in surface production, disturbance by lateral water intrusions, and their combination. However, temporal dynamics of bacterial community composition are complicated, and they are only weakly related to

contemporaneously measured environmental parameters. Our semiannual sampling frequency is certainly inadequate to observe real-time responses of bacterial communities to environmental changes. Therefore, long-term variability in marine microbial communities, at least in the Cariaco Basin, is hard to understand from community snapshots with relatively low sampling frequency.

References

- AMANN, R. I., B. J. BINDER, R. J. OLSON, S. W. CHISHOLM, R. DEVEREUX, AND D. A. STAHL. 1990. Combination of 16S ribosomal-RNA-targeted oligonucleotide probes with flow-cytometry for analyzing mixed microbial populations. *App. Environ. Microbiol.* **56**: 1919–1925.
- ASTOR, Y., F. MULLER-KARGER, AND M. SCRANTON. 2003. Seasonal and interannual variation in the hydrography of the Cariaco Basin: Implications for basin ventilation. *Cont. Shelf Res.* **23**: 125–144.
- BLACKWOOD, C., T. MARSH, S. KIM, AND E. PAUL. 2003. Terminal restriction fragment length polymorphism data analysis for quantitative comparison of microbial communities. *Appl. Environ. Microbiol.* **69**: 926–932.
- BUCKLING, A., R. KASSEN, G. BELL, AND P. RAINEY. 2000. Disturbance and diversity in experimental microcosms. *Nature* **408**: 961–964.
- BURKERT, U., F. WARNECKE, D. BABENZIEN, E. ZWIRNMANN, AND J. PERNTHALER. 2003. Members of a readily enriched beta-proteobacterial clade are common in surface waters of a humic lake. *Appl. Environ. Microbiol.* **69**: 6550–6559.
- CHISTOSERDOVA, L., M. KALYUZHNAJA, AND M. LIDSTROM. 2005. C-1-transfer modules: From genomics to ecology. *ASM News* **71**: 521–526.
- DAVISON, W., D. WOOF, AND E. RIGG. 1982. The dynamics of iron and manganese in a seasonally anoxic lake: Direct measurement of fluxes using sediment traps. *Limnol. Oceanogr.* **27**: 987–1003.
- DE'ATH, G. 1999. Principal curves: A new technique for indirect and direct gradient analysis. *Ecology* **80**: 2237–2253.
- FUHRMAN, J., I. HEWSON, M. SCHWALBACH, J. STEELE, M. BROWN, AND S. NAEEM. 2006. Annually reoccurring bacterial communities are predictable from ocean conditions. *PNAS* **103**: 13104–13109.
- GHIGLIONE, J., M. LARCHER, AND P. LEBARON. 2005. Spatial and temporal scales of variation in bacterioplankton community structure in the NW Mediterranean Sea. *Aquat. Microb. Ecol.* **40**: 229–240.
- GIOVANNONI, S., M. RAPPE, D. GORDON, E. URBACH, M. SUZUKI, AND K. FIELD. 1996. Ribosomal RNA and the evolution of bacterial diversity, p. 63–85. *In* D. M. Roberts, P. Sharp, G. Alderson and M. Collins [eds.], *Evolution of microbial life*. Cambridge Univ. Press.
- HANSON, R., AND T. HANSON. 1996. Methanotrophic bacteria. *Microbiol. Rev.* **60**: 439–471.
- HAYES, M. K., G. T. TAYLOR, Y. ASTOR, AND M. I. SCRANTON. 2006. Vertical distributions of thiosulfate and sulfite in the Cariaco Basin. *Limnol. Oceanogr.* **51**: 280–287.
- HO, T., G. TAYLOR, Y. ASTOR, R. VARELA, F. MULLER-KARGER, AND M. SCRANTON. 2004. Vertical and temporal variability of redox zonation in the water column of the Cariaco Basin: Implications for organic carbon oxidation pathways. *Mar. Chem.* **86**: 89–104.
- HUISMAN, J., N. THI, D. KARL, AND B. SOMMEIJER. 2006. Reduced mixing generates oscillations and chaos in the oceanic deep chlorophyll maximum. *Nature* **439**: 322–325.
- HUNTER-CEVERA, J., D. KARL, AND A. BUCKLEY. 2005. Marine microbial diversity: The key to Earth's habitability. A report from the American Academy of Microbiology. American Society for Microbiology.
- KESSLER, J., W. REEBURGH, J. SOUTHON, AND R. VARELA. 2005. Fossil methane source dominates Cariaco Basin water column methane geochemistry. *Geophys. Res. Lett.* **32**: L12609, doi:10.1029/2005GL022984.
- KONOPKA, A. 2006. Microbial ecology: Searching for principles. *Microbe* **1**: 175–179.
- LABRENZ, M., G. JOST, C. POHL, S. BECKMANN, W. MARTENS-HABBENA, AND K. JURGENS. 2005. Impact of different in vitro electron donor/acceptor conditions on potential chemolithoautotrophic communities from marine pelagic redox-clines. *Appl. Environ. Microbiol.* **71**: 6664–6672.
- LIN, X., M. SCRANTON, R. VARELA, A. CHISTOSERDOV, AND G. TAYLOR. 2007. Compositional responses of bacterial communities to redox gradients and grazing in the anoxic Cariaco Basin. *Aquat. Microb. Ecol.* **47**: 57–72.
- , S. WAKEHAM, I. PUTNAM, Y. ASTOR, M. SCRANTON, A. CHISTOSERDOV, AND G. TAYLOR. 2006. Vertical distributions of prokaryotic assemblages in the anoxic Cariaco Basin and Black Sea compared using fluorescence in situ hybridization (FISH). *Appl. Environ. Microbiol.* **72**: 2679–2690.
- LOREAU, M. 1998. Biodiversity and ecosystem functioning: A mechanistic model. *Proc. Natl. Acad. Sci. USA* **95**: 5632–5636.
- MADRID, V., G. TAYLOR, M. SCRANTON, AND A. CHISTOSERDOV. 2001. Phylogenetic diversity of bacterial and archaeal communities in the anoxic zone of the Cariaco Basin. *Appl. Environ. Microbiol.* **67**: 1663–1674.
- MADSEN, E. 2005. Identifying microorganisms responsible for ecologically significant biogeochemical processes. *Nature Rev. Microbiol.* **3**: 439–446.
- MANZ, W., R. AMANN, W. LUDWIG, M. VANCANNEYT, AND K. SCHLEIFER. 1996. Application of a suite of 16S rRNA-specific oligonucleotide probes designed to investigate bacteria of the phylum *cytophaga-flavobacter-bacteroides* in the natural environment. *Microbiology-UK* **142**: 1097–1106.
- , R. I. AMANN, W. LUDWIG, M. WAGNER, AND K. H. SCHLEIFER. 1992. Phylogenetic oligodeoxynucleotide probes for the major subclasses of proteobacteria—problems and solutions. *Syst. Appl. Microbiol.* **15**: 593–600.
- MARCHESE, J., T. SATO, A. WEIGHTMAN, T. MARTIN, J. FRY, S. HIOM, D. DYMCK, AND W. WADE. 1998. Design and evaluation of useful bacterium-specific PCR primers that amplify genes coding for bacterial 16S rRNA. *Appl. Environ. Microbiol.* **64**: 795–799.
- MCCUNE, B., AND J. B. GRACE. 2002. Analysis of ecological communities. *MJM Software Design*.
- MOESENEDER, M., J. ARRIETA, G. MUYZER, C. WINTER, AND G. HERNDL. 1999. Optimization of terminal-restriction fragment length polymorphism analysis for complex marine bacterioplankton communities and comparison with denaturing gradient gel electrophoresis. *Appl. Environ. Microbiol.* **65**: 3518–3525.
- MULLER-KARGER, F., R. VARELA, R. THUNELL, M. SCRANTON, R. BOHRER, G. TAYLOR, J. CAPELO, Y. ASTOR, E. TAPPA, T. HO, AND J. WALSH. 2001. Annual cycle of primary production in the Cariaco Basin: Response to upwelling and implications for vertical export. *J. Geophys. Res.* **106**: 4527–4542.
- NEEF, A. 1997. Anwendung der in situ Einzelzell-Identifizierung von Bakterien zur Populationsanalyse in komplexen mikrobiellen Biozönosen. Ph.D. thesis, Technische Universität München.

- NOLD, S. C., AND G. ZWART. 1998. Patterns and governing forces in aquatic microbial communities. *Aquat. Ecol.* **32**: 17–35.
- OGUZ, T., J. MURRAY, AND A. CALLAHAN. 2001. Modeling redox cycling across the suboxic–anoxic interface zone in the Black Sea. *Deep-Sea Res. I* **48**: 761–787.
- PERCY, D., X. LI, G. T. TAYLOR, Y. ASTOR, AND M. I. SCRANTON. In press. Controls on iron, manganese and intermediate oxidation state sulfur compounds in the Cariaco Basin. *Mar. Chem.*
- PERNTHALER, J., AND R. AMANN. 2005. Fate of heterotrophic microbes in pelagic habitats: Focus on populations. *Microbiol. Mol. Biol. Rev.* **69**: 440–461.
- PETT-RIDGE, J., AND M. FIRESTONE. 2005. Redox fluctuation structures microbial communities in a wet tropical soil. *Appl. Environ. Microbiol.* **71**: 6998–7007.
- PORTER, K., AND Y. FEIG. 1980. The use of DAPI for identification and counting aquatic microflora. *Limnol. Oceanogr.* **25**: 943–948.
- RICHARDS, F. A. 1975. The Cariaco Basin (Trench). *Oceanogr. Mar. Bio. Ann. Rev.* **13**: 11–67.
- SCRANTON, M., Y. ASTOR, R. BOHRER, T. HO, AND F. MULLER-KARGER. 2001. Controls on temporal variability of the geochemistry of the deep Cariaco Basin. *Deep-Sea Res. I* **48**: 1605–1625.
- , F. SAYLES, M. BACON, AND P. BREWER. 1987. Temporal changes in the hydrography and chemistry of the Cariaco Trench. *Deep-Sea Res. I* **34**: 945–963.
- SCRANTON, M. I., G. T. TAYLOR, Y. ASTOR, AND F. MULLER-KARGER. 2006. Temporal variability in the nutrient chemistry of the Cariaco Basin, p. 139–160. *In* L. N. Neretin [ed.], *Past and present water column anoxia*. NATO Sci. Ser. Springer.
- SUZUKI, M., C. PRESTON, F. CHAVEZ, AND E. DELONG. 2001. Quantitative mapping of bacterioplankton populations in seawater: Field tests across an upwelling plume in Monterey Bay. *Aquat. Microb. Ecol.* **24**: 117–127.
- TAYLOR, G., M. IABICHELLA, T. HO, M. SCRANTON, R. THUNELL, F. MULLER-KARGER, AND R. VARELA. 2001. Chemoautotrophy in the redox transition zone of the Cariaco Basin: A significant midwater source of organic carbon production. *Limnol. Oceanogr.* **46**: 148–163.
- TAYLOR, G. T., M. IABICHELLA, R. VARELA, F. MULLER-KARGER, X. LIN, AND M. I. SCRANTON. 2006. Microbial ecology of the Cariaco Basin's redoxcline: The U.S.–Venezuela CARIACO time series program, p. 473–499. *In* L. N. Neretin [ed.], *Past and present water column anoxia*. NATO Sci. Ser., Springer.
- VETRIANI, C., H. TRAN, AND L. KERKHOF. 2003. Fingerprinting microbial assemblages from the oxic/anoxic chemocline of the Black Sea. *Appl. Environ. Microbiol.* **69**: 6481–6488.
- WALLNER, G., R. AMANN, AND W. BEISKER. 1993. Optimizing fluorescent in situ hybridization with ribosomal-RNA-targeted oligonucleotide probes for flow cytometric identification of microorganisms. *Cytometry* **14**: 136–143.
- WARD, B. 2005. Molecular approaches to marine microbial ecology and the marine nitrogen cycle. *Ann. Rev. Earth Planet. Sci.* **33**: 301–333.
- , K. KILPATRICK, P. NOVELLI, AND M. SCRANTON. 1987. Methane oxidation and methane fluxes in the ocean surface-layer and deep anoxic waters. *Nature* **327**: 226–229.
- YILMAZ, L., AND D. NOGUERA. 2004. Mechanistic approach to the problem of hybridization efficiency in fluorescent in situ hybridization. *Appl. Environ. Microbiol.* **70**: 7126–7139.

Received: 2 February 2007
Accepted: 19 June 2007
Amended: 23 July 2007